CMS-Flux-NA Fluxes and Aircraft CO2 Co-samples for 2018-2019

Get Data

Documentation Revision Date: 2024-04-24

Dataset Version: 1

Summary

This dataset provides gridded surface-atmosphere CO2 fluxes over North America from April 8 to November 18 during 2018 and 2019. Net ecosystem exchange (NEE) was estimated by the CMS-Flux-NA CO2 inversion system by assimilating in situ CO2 measurements and/or Orbiting Carbon Observatory (OCO-2) column-averaged CO2 retrievals. These data, along with imposed diurnal NEE variations, fossil fuel emissions, biomass burning, and biofuel emissions, are provided at 3-hour temporal resolution. The modeled co-samples of CO2 observed for aircraft flights are included for model evaluation. The data are provided in NetCDF version 4 format.

There are 22 files in NetCDF version 4 format (.nc) in this dataset.

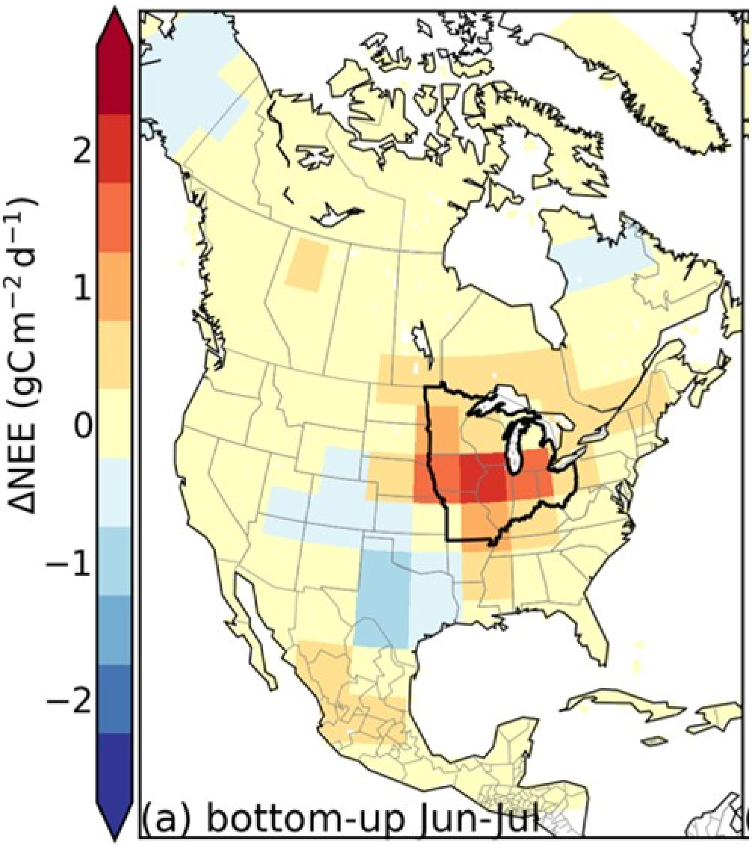

Figure 1. Bottom-up (LNLGOGIS) spatial patterns of June-July mean change in net ecosystem exchange (NEE_2019-NEE_2018) at 4 x 5-degrees spatial resolution.

Citation

Byrne, B.K., J. Liu, K.W. Bowman, Y. Yin, J. Yun, G. Ferreira, S.M. Ogle, L. Baskaran, L. He, X. Li, J. Xiao, and K.J. Davis. 2024. CMS-Flux-NA Fluxes and Aircraft CO2 Co-samples for 2018-2019. ORNL DAAC, Oak Ridge, Tennessee, USA. https://doi.org/10.3334/ORNLDAAC/2336

Table of Contents

1. Dataset Overview

Project: Carbon Monitoring System

The NASA Carbon Monitoring System (CMS) program is designed to make significant contributions in characterizing, quantifying, understanding, and predicting the evolution of global carbon sources and sinks through improved monitoring of carbon stocks and fluxes. The System uses NASA satellite observations and modeling/analysis capabilities to establish the accuracy, quantitative uncertainties, and utility of products for supporting national and international policy, regulatory, and management activities. CMS data products are designed to inform near-term policy development and planning.

Related Publication

Byrne, B., J. Liu, K.W. Bowman, Y. Yin, J. Yun, G. Ferreira, S. Ogle, L. Baskaran, L. He, X. Li, J. Xiao, and K.J. Davis. 2024. Regional inversion shows promise in capturing extreme-event-driven CO2 flux anomalies but is limited by atmospheric CO2 observational coverage. Journal of Geophysical Research: Atmospheres, 129, e2023JD040006. https://doi.org/10.1029/2023JD040006

Related Dataset

Davis, K.J., M.D. Obland, B. Lin, T. Lauvaux, C. O'Dell, B. Meadows, E.V. Browell, J.P. DiGangi, C. Sweeney, M.J. McGill, J.D. Barrick, A.R. Nehrir, M.M. Yang, J.R. Bennett, B.C. Baier, A. Roiger, S. Pal, T. Gerken, A. Fried, S. Feng, R. Shrestha, M.A. Shook, G. Chen, L.J. Campbell, Z.R. Barkley, and R.M. Pauly. 2018. ACT-America: L3 Merged In Situ Atmospheric Trace Gases and Flask Data, Eastern USA. ORNL DAAC, Oak Ridge, Tennessee, USA. https://doi.org/10.3334/ORNLDAAC/1593

Acknowledgement

This study was supported with the following grants: NASA's Carbon Monitoring System (CMS, grants 80NSSC21K1060 and 80NM0018F0583); NASA's Orbiting Carbon Observatory (OCO) science team (grant 80NM0018F0583); and the National Science Foundation's Macrosystems Biology and NEON-Enabled Science (MSB-NES) program (grant DEB-2017870).

2. Data Characteristics

Spatial Coverage: North America

Spatial Resolution: 0.500 x 0.625 degrees

Temporal Coverage: 2018-01-01 to 2019-12-31 prior fluxes, 2018-04-08 to 2018-11-18, 2019-04-08 to 2019-11-18 for inversion analyses

Temporal Resolution: 3-hourly

Study Areas: Latitude and longitude are given in decimal degrees.

Site	Westernmost Longitude	Easternmost Longitude	Northernmost Latitude	Southernmost Latitude
North America	-167.8125	-39.6875	76.250	13.750

Data File Information

There are 22 data files in NetCDF (.nc) format with this dataset.

There are five types of files:

1. ***NorthAmerica_<YYYY>_<experiment>.nc*** : modeled surface-atmosphere CO_2 fluxes for the standard experiment for a given year. Each file contains CO_2 fluxes (net ecosystem exchange, NEE) at 3-h intervals using the climatological prior NEE (SiB3, CASA and FLUXCOM) and posterior NEE (SiB3, CASA and FLUXCOM using priors). Files also include emissions from fossil fuels use, biofuels use, and biomass burning (Table 1). Eight files.
2. ***NorthAmerica_Prior_Fluxes.nc*** : Prior fluxes and uncertainties for the standard experiment. Values are weekly averages over one year (n=52) (Table 2).
3. ***NorthAmerica_<YYYY>_<experiment>_wPriorIAV.nc*** : modeled surface-atmosphere CO_2 fluxes for the experiment using priors with interannual variability (IAV) for a given year (Table 2). Files have the same structure as the standard experiment (1). Eight files.
4. ***<experiment>_aircraft_cosamples.nc*** : observed in-situ and simulated co-samples of aircraft CO_2 measurements for the standard experiment (Table 3). Four files.
5. ***Prior_aircraft_cosamples.nc** :* aircraft CO_2 co-samples simulated using prior fluxes without performing optimization (Table 3).

For *NorthAmerica_<YYYY>_<experiment>.nc, NorthAmerica_<YYYY>_<experiment>_wPriorIAV.nc,* and *<experiment>_aircraft_cosamples.nc***,**

- *<YYYY>* is the year (2018 or 2019)
- *<experiment>* is the type of inversion: ("IS", "LNLG", "LNLGIS", or "LNLGOGIS"). See Section 5 for explanation.

Table 1. Variables in *NorthAmerica_<YYYY>_<experiment>.nc* and *NorthAmerica_<YYYY>_<experiment>_wPriorIAV.nc* files.

Variable	Units	Description
time	d	Fractional days since 2018-01-01 00:00:00; time step is 0.125 d (3 h)

lat	degrees east	Latitude for center of grid cell
lon	degrees north	Longitude for center of grid cell
area	m^2	Grid cell area
posterior_CASA_NEE	g m^{-2} day^{-1}	Posterior net ecosystem exchange (NEE) in grams carbon from inversion using the CASA prior
posterior_SiB3_NEE	g m^{-2} day^{-1}	Posterior NEE in grams carbon from inversion using the SiB3 prior
posterior_FLUXCOM_NEE	g m^{-2} day^{-1}	Posterior NEE in grams carbon from inversion using the FLUXCOM prior
prior_CASA_NEE*	g m^{-2} day^{-1}	Prior for CASA NEE in grams carbon
prior_SiB3_NEE*	g m^{-2} day^{-1}	Prior for SiB3 NEE in grams carbon
prior_FLUXCOM_NEE*	g m^{-2} day^{-1}	Prior for FLUXCOM NEE in grams carbon
Fossil_Fuels	g m^{-2} day^{-1}	Fossil fuel CO_2 emissions in grams carbon
Biomass_Burning	g m^{-2} day^{-1}	Biomass burning CO_2 emissions in grams carbon
Biofuels	g m^{-2} day^{-1}	Biofuel CO_2 emissions in grams carbon

*NEE priors were obtained from Byrne et al. (2020).

Table 2. Variables in *NorthAmerica_Prior_Fluxes.nc*.

Variable	Units	Description
time	d	Mid-point of week over one year (n=52); time step is 1 week (7 days) and units are fractional days
lat	degrees east	Latitude for center of grid cell
lon	degrees north	Longitude for center of grid cell
area	m^2	Area of grid cell
mask	1	Region mask ID; values relate lat-lon grid to state vector
NPP	g m^{-2} day^{-1}	Prior for net primary production
HR_FLUXCOM	g m^{-2} day^{-1}	Prior for heterotrophic respiration (NEE_GIT_FLUXCOM - NPP) in grams carbon
HR_UNC_FLUXCOM	g m^{-2} day^{-1}	Uncertainty on HR_FLUXCOM
HR_CASA	g m^{-2} day^{-1}	Prior for heterotrophic respiration (NEE_GIT_CASA - NPP) in grams carbon
HR_UNC_CASA	g m^{-2} day^{-1}	Uncertainty on HR_CASA
HR_SiB3	g m^{-2} day^{-1}	Prior for heterotrophic respiration (NEE_GIT_SiB3 - NPP) in grams carbon
HR_UNC_SiB3	g m^{-2} day^{-1}	Uncertainty on HR_SiB3
ocean_FLUXCOM*	g m^{-2} day^{-1}	Prior for ocean-atmosphere CO_2 flux in grams carbon
ocean_UNC_FLUXCOM	g m^{-2} day^{-1}	Uncertainty on ocean_FLUXCOM
ocean_CASA*	g m^{-2} day^{-1}	Prior for ocean-atmosphere CO_2 flux in grams carbon
ocean_UNC_CASA	g m^{-2} day^{-1}	Uncertainty on ocean_CASA
ocean_SiB3*	g m^{-2} day^{-1}	Prior for ocean-atmosphere CO_2 flux in grams carbon
ocean_UNC_SiB3	g m^{-2} day^{-1}	Uncertainty on ocean_SiB3

*Priors obtained from GOSAT+surface+TCCON (GIT) experiments in Byrne et al. (2020).

Table 3. Variables in *<experiment>_aircraft_cosamples.nc* files and *Prior_aircraft_cosamples.nc*.

Variable	Units	Description
time	h	Time in fractional hours since 2018-01-01 00:00:00
obspack_id	-	Unique identifier of measurement from Obspack dataset
year	y	Calendar year of in situ sample

month	month	Month of year (range: 1-12) of in situ sample
dat_of_month	d	Day of month (range: 1-31) of in situ sample
doy	d	Day of year (range: 1-365) in situ sample
hour	h	Fractional hour of day (0.00 - 23.99) of in situ sample
lat	degrees east	Latitude for center of grid cell
lon	degrees north	Longitude for center of grid cell
Y	ppm	Observed mole fraction of CO_2 in dry air in ppm
HX_SiB3	ppm	Posterior simulated mole fraction of CO_2 (based on SiB3 prior)
HX_CASA	ppm	Posterior simulated mole fraction of CO_2 (based on CASA prior)
HX_FLUXCOM	ppm	Posterior simulated mole fraction of CO_2 (based on FLUXCOM prior)
height	m	Aircraft height (altitude) above the surface
site_num	-	Unique number for aircraft campaign

3. Application and Derivation

These data provide posterior NEE estimates and posterior CO_2 co-samples from the nested CMS-Flux-NA inversion system. The fluxes provided here can be used to study CO_2 fluxes over North America (e.g., Figure 2). Atmospheric CO_2 inversion analyses are most robust over larger spatial-temporal scales; therefore, limiting analysis to scales of monthly temporal duration and spatial scales of ≥1000 km is recommended.

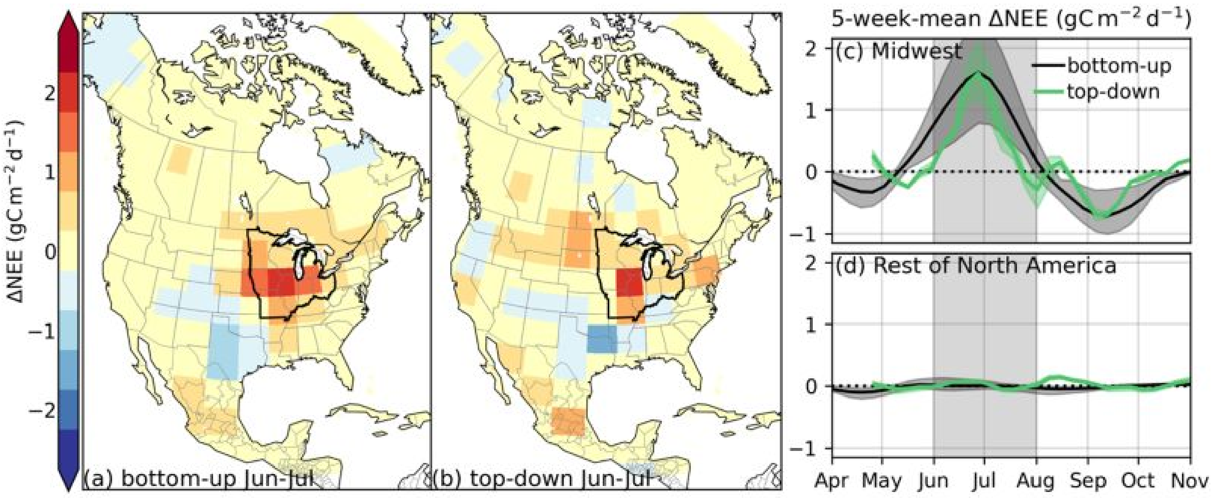

Figure 2. (a) Bottom-up and (b) top-down (LNLGOGIS) spatial patterns of June–July mean change in NEE (NEE2019 − NEE2018) at 4 × 5-degree spatial resolution. (c) US Midwest and (d) rest of North America 5-week-mean change in NEE. The US Midwest is defined as the area within Illinois, Indiana, Iowa, Michigan, Minnesota, Missouri, Ohio, and Wisconsin and is indicated by the black outline in panels (a) and (b). The shading shows the range around the mean estimate for the inversions using three different priors and for the five bottom-up GPP datasets. Source: Byrne et al. (2024).

4. Quality Assessment

Fluxes were evaluated through comparisons of posterior simulated CO_2 concentrations with aircraft CO_2 measurements that were not assimilated in the inversions. These co-sample data are also provided here for further analysis. A rough estimate of uncertainty can be obtained through examining the spread in flux estimates resulting from the three different prior NEE models (CASA, SiB3 and FLUXCOM). See Byrne et al. (2024) for a description of this comparison.

5. Data Acquisition, Materials, and Methods

Atmospheric CO_2 inversions were performed with the CMS-Flux-NA model for North America for the months of April to November in 2018 and 2019. The set-up of this inversion system is described in detail in Byrne et al. (2024). In short, atmospheric CO_2 data was assimilated using Bayesian inference to optimize weekly CO_2 fluxes for land and ocean. Rather than directly optimizing land NEE, the inversion optimized heterotrophic respiration (HR) fluxes that were then combined with prescribed net primary production (NPP) to generate NEE. This approach improved inversion performance, and the component HR and NPP fluxes were not examined. Individual inversions were six weeks long with the first and last week discarded as spin-up/spin-down. A batch of eight six-week inversions, shifted by four weeks, were conducted to cover the entire April 8 to Nov 18 period.

Results for two ensembles of inversions are provided in this dataset. The “standard” experiment is for inversions with climatological prior NEE while the “IAV” experiment has interannual variations in prior NEE. A tree diagram illustrating the 12 individual inversions shown for the “standard” experiment are shown in Figure 3. The diagram shows that four sets of inversions are conducted that differ in assimilated data:

- The “IS” inversions assimilate in situ CO_2 measurements from the global network of sites.
- The “LNLG” inversions assimilate OCO-2 land data, including nadir and glint retrievals.

- The “LNLGIS” inversions assimilate both in situ and OCO-2 land data.
- The “LNLGOGIS” inversions assimilate in situ, OCO-2 land data, and OCO-2 ocean glint retrievals.

For each assimilated dataset, three sets of inversions differing in prior fluxes are conducted. These prior NEE estimates were obtained from the GOSAT+surface+TCCON (GIT) experiment of Byrne et al. (2020). These NEE estimates are themselves posterior NEE estimates from inversions that assimilated GOSAT column-averaged dry-air mole fraction (XCO2) retrievals, surface in situ CO_2, and TCCON XCO2 in a global inversion over 2010–2015. The three different NEE estimates differ based on prior fluxes used in the inversions, either CASA, SiB3 or FLUXCOM NEE.

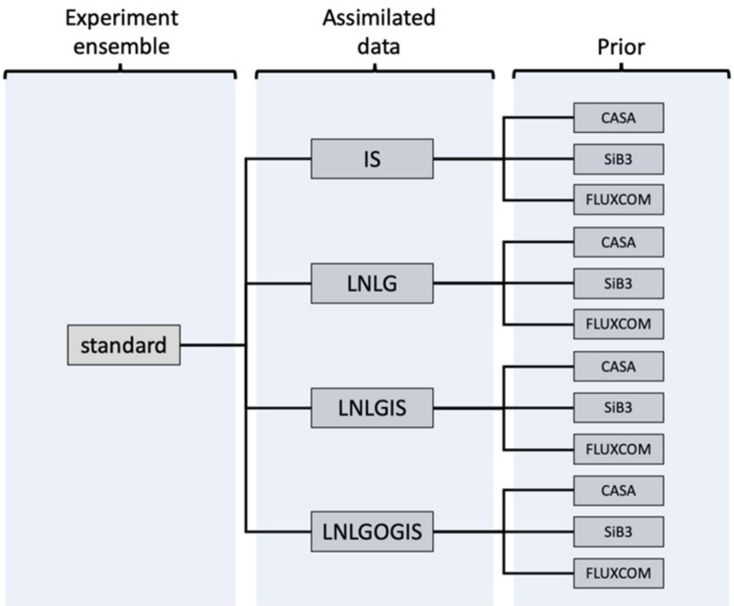

Figure 3. Tree diagram showing the 12 inversions conducted for the standard experiment ensemble. For a given experiment, sub-experiments that assimilate different observation using each prior NEE are performed.

Assimilated data

In situ CO_2 measurements are obtained from version 8.0 of the NOAA GLOBALVIEW plus Obspack dataset (Schuldt et al., 2022). These data are provided on the X2019 CO2 scale but were back corrected to the X2007 CO2 scale following Hall et al. (2021). Several filters were applied to the in situ data before assimilation. Surface in situ CO_2 measurements are assimilated at their respective height above the surface, with inclusion criteria that the model surface elevation should differ by less than 500 m from the 15 arc-second ETOPO1 global elevation dataset (NOAA, 2022) (to exclude observations whose elevation differs significantly from the model grid). Secondly, only assimilate data with the CT assim flag greater than or equal to one, which indicates data that is deemed assimilable for the NOAA CarbonTracker system. Finally, only measurements obtained between 11:00 and 17:00 local time are assimilated (when the atmospheric boundary layer is well mixed). The sites assimilated were: amt, bck, bmw, bra, brw, cba, cby, chl, cps, crv, egb, esp, est, etl, fsd, inu, inx, key, kum, lef, lew, llb, sct, sgp, uta, wbi, wgc, wkt, wsa. The sites with CT assim≥ 1 that are not assimilated were: mbo, mex, mlo, mwo, nwr, omp, uts, wsd. Some sites with CT assim= 0 may be assimilable, but more work is needed to characterize their suitability for assimilation.The CT MDM “model-data-mismatch” values were applied as uncertainties on assimilated measurements. All aircraft data, including the ACT-America campaign data (Davis et al., 2021, 2018; Wei et al., 2021), were withheld for validation purposes

XCO2 data were retrieved using version 10 of NASA’s Atmospheric CO2 Observations from Space (ACOS) full-physics retrieval algorithm (O’Dell et al., 2018). Subsequently, OCO-2 “buddy” super-observations were calculated by averaging individual soundings into super-observations at a spatial resolution of 0.5 × 0.5 degree within the same orbit, assigning equal weights, following the approach by Liu et al. (2017).

See Byrne et al. (2024) for additional details.

6. Data Access

These data are available through the Oak Ridge National Laboratory (ORNL) Distributed Active Archive Center (DAAC).

CMS-Flux-NA Fluxes and Aircraft CO2 Co-samples for 2018-2019

Contact for Data Center Access Information:

- E-mail: uso@daac.ornl.gov
- Telephone: +1 (865) 241-3952

7. References

Byrne, B., J. Liu, K.W. Bowman, Y. Yin, J. Yun, G. Ferreira, S. Ogle, L. Baskaran, L. He, X. Li, J. Xiao, and K.J. Davis. 2024. Regional inversion shows promise in capturing extreme-event-driven CO2 flux anomalies but is limited by atmospheric CO2 observational coverage. Journal of Geophysical Research: Atmospheres, 129, e2023JD040006. https://doi.org/10.1029/2023JD040006

Byrne, B., J. Liu, M. Lee, I. Baker, K.W. Bowman, N.M. Deutscher, D.G. Feist, D.W. T. Griffith, L.T. Iraci, M. Kiel, J.S. Kimball, C.E. Miller, I. Morino, N.C. Parazoo, C. Petri, C.M. Roehl, M.K. Sha, K. Strong, V.A. Velazco, P.O. Wennberg, and D. Wunch. 2020. Improved constraints on northern extratropical CO2 fluxes obtained by combining surface-based and space-based atmospheric CO2 measurements. Journal of Geophysical Research: Atmospheres 125:e2019JD032029. https://doi.org/10.1029/2019JD032029

Davis, K.J., E.V. Browell, S. Feng, T. Lauvaux, M.D. Obland, S. Pal, B.C. Baier, D.F. Baker, I.T. Baker, Z.R. Barkley, K.W. Bowman, Y.Y. Cui, A.S. Denning, J.P. DiGangi, J.T. Dobler, A. Fried, T. Gerken, K. Keller, B. Lin, A.R. Nehrir, C.P. Normile, C.W. O’Dell, L.E. Ott, A. Roiger, A.E. Schuh, C. Sweeney, Y. Wei, B. Weir, M. Xue, and C.A. Williams. 2021. The Atmospheric Carbon and Transport (ACT)-America Mission. Bulletin of the American

Meteorological Society 102:E1714–E1734. https://doi.org/10.1175/BAMS-D-20-0300.1

Davis, K.J., M.D. Obland, B. Lin, T. Lauvaux, C. O'Dell, B. Meadows, E.V. Browell, J.P. DiGangi, C. Sweeney, M.J. McGill, J.D. Barrick, A.R. Nehrir, M.M. Yang, J.R. Bennett, B.C. Baier, A. Roiger, S. Pal, T. Gerken, A. Fried, S. Feng, R. Shrestha, M.A. Shook, G. Chen, L.J. Campbell, Z.R. Barkley, and R.M. Pauly. 2018, June 25. ACT-America: L3 Merged In Situ Atmospheric Trace Gases and Flask Data, Eastern USA. ORNL Distributed Active Archive Center. https://doi.org/10.3334/ORNLDAAC/1593

Hall, B.D., A.M. Crotwell, D.R. Kitzis, T. Mefford, B.R. Miller, M.F. Schibig, and P.P. Tans. 2021. Revision of the World Meteorological Organization Global Atmosphere Watch (WMO/GAW) CO_2 calibration scale. Atmospheric Measurement Techniques 14:3015–3032. https://doi.org/10.5194/amt-14-3015-2021

Liu, J., K.W. Bowman, D.S. Schimel, N.C. Parazoo, Z. Jiang, M. Lee, A.A. Bloom, D. Wunch, C. Frankenberg, Y. Sun, C.W. O'Dell, K.R. Gurney, D. Menemenlis, M. Gierach, D. Crisp, and A. Eldering. 2017. Contrasting carbon cycle responses of the tropical continents to the 2015–2016 El Niño. Science 358. http://doi.org/10.1126/science.aam5690

NOAA National Centers for Environmental Information. 2022. ETOPO 2022 15 Arc-Second Global Relief Model. NOAA National Centers for Environmental Information. https://doi.org/10.25921/fd45-gt74

O'Dell, C.W., A. Eldering, P.O. Wennberg, D. Crisp, M.R. Gunson, B. Fisher, C. Frankenberg, M. Kiel, H. Lindqvist, L. Mandrake, A. Merrelli, V. Natraj, R.R. Nelson, G.B. Osterman, V.H. Payne, T.E. Taylor, D. Wunch, B.J. Drouin, F. Oyafuso, A. Chang, J. McDuffie, M. Smyth, D.F. Baker, S. Basu, F. Chevallier, S.M. R. Crowell, L. Feng, P.I. Palmer, M. Dubey, O.E. García, D.W. T. Griffith, F. Hase, L.T. Iraci, R. Kivi, I. Morino, J. Notholt, H. Ohyama, C. Petri, C.M. Roehl, M.K. Sha, K. Strong, R. Sussmann, Y. Te, O. Uchino, and V.A. Velazco. 2018. Improved retrievals of carbon dioxide from Orbiting Carbon Observatory-2 with the version 8 ACOS algorithm. Atmospheric Measurement Techniques 11:6539–6576. https://doi.org/10.5194/amt-11-6539-2018

Schuldt, K.N., J. Mund, I.T. Luijkx, T. Aalto, J.B. Abshire, K. Aikin, Arlyn Andrews, S. Aoki, F. Apadula, B. Baier, P. Bakwin, J. Bartyzel, G. Bentz, P. Bergamaschi, A. Beyersdorf, T. Biermann, S.C. Biraud, H. Boenisch, D. Bowling, G. Brailsford, W.A. Brand, P. Van Den Bulk, G. Chen, Huilin Chen, Lukasz Chmura, S. Clark, Sites Climadat, J.D. Coletta, A. Colomb, R. Commane, S. Conil, C. Couret, A. Cox, P. Cristofanelli, E. Cuevas, R. Curcoll, B. Daube, K. Davis, M. Delmotte, J.P. DiGangi, D. Van Dinther, E. Dlugokencky, J.W. Elkins, L. Emmenegger, Shuangxi Fang, M.L. Fischer, G. Forster, A. Frumau, M. Galkowski, L.V. Gatti, T. Gehrlein, C. Gerbig, Francois Gheusi, E. Gloor, V. Gomez-Trueba, D. Goto, T. Griffis, S. Hammer, C. Hanson, L. Haszpra, J. Hatakka, M. Heimann, M. Heimann, M. Heliasz, D. Heltai, A. Hensen, O. Hermanssen, E. Hintsa, A. Hoheisel, J. Holst, V. Ivakhov, D. Jaffe, A. Jordan, W. Joubert, A. Karion, S.R. Kawa, V. Kazan, R. Keeling, P. Keronen, Jooil Kim, T. Kneuer, P. Kolari, K. Kominkova, E. Kort, E. Kozlova, P. Krummel, D. Kubistin, C. Labuschagne, D.H. Y. Lam, X. Lan, R. Langenfelds, O. Laurent, T. Laurila, T. Lauvaux, J. Lavric, B. Law, J. Lee, O.S. M. Lee, I. Lehner, K. Lehtinen, R. Leppert, A. Leskinen, M. Leuenberger, I. Levin, J. Levula, J. Lin, M. Lindauer, Z. Loh, M. Lopez, C.R. Lunder, T. Machida, I. Mammarella, G. Manca, A. Manning, A. Manning, M.V. Marek, M.Y. Martin, Giordane A. Martins, H. Matsueda, M. De Mazière, K. McKain, H. Meijer, F. Meinhardt, L. Merchant, N. Mihalopoulos, N. Miles, C.E. Miller, J.B. Miller, L. Mitchell, M. Mölder, S. Montzka, F. Moore, H. Moossen, E. Morgan, Josep-Anton Morgui, S. Morimoto, J. Müller-Williams, B. Munger, D. Munro, C.L. Myhre, Jaroslaw Necki, S. Newman, S. Nichol, Y. Niwa, S. O'Doherty, F. Obersteiner, B. Paplawsky, J. Peischl, O. Peltola, S. Piacentino, J.M. Pichon, S. Piper, J. Pitt, C. Plass-Duelmer, C. Plass-Duelmer, S.M. Platt, S. Prinzivalli, M. Ramonet, R. Ramos, E. Reyes-Sanchez, S. Richardson, H. Riris, P.P. Rivas, M. Rothe, T. Ryerson, K. Saito, M. Sargent, A.G. Di Sarra, M. Sasakawa, B. Scheeren, M. Schmidt, T. Schuck, M. Schumacher, T. Seifert, M.K. Sha, P. Shepson, M. Shook, C.D. Sloop, P. Smith, L.L. Sørensen, R.A. F. De Souza, M. Steinbacher, B. Stephens, C. Sweeney, P. Tans, K. Thoning, H. Timas, M. Torn, K. Tørseth, P. Trisolino, J. Turnbull, A. Vermeulen, B. Viner, G. Vitkova, S. Walker, A. Watson, R. Weiss, S. De Wekker, S. Wofsy, J. Worsey, D. Worthy, Dickon Young, S. Zaehle, A. Zahn, and Miroslaw Zimnoch. 2022. Multi-laboratory compilation of atmospheric carbon dioxide data for the period 1957-2021; obspack_co2_1_GLOBALVIEWplus_v8.0_2022-08-27. NOAA Global Monitoring Laboratory. https://doi.org/10.25925/20220808

Wei, Y., R. Shrestha, S. Pal, T. Gerken, S. Feng, J. McNelis, D. Singh, M.M. Thornton, A.G. Boyer, M.A. Shook, G. Chen, B.C. Baier, Z.R. Barkley, J.D. Barrick, J.R. Bennett, E.V. Browell, J.F. Campbell, L.J. Campbell, Y. Choi, J. Collins, J. Dobler, M. Eckl, A. Fiehn, A. Fried, J.P. Digangi, R. Barton-Grimley, H. Halliday, T. Klausner, S. Kooi, J. Kostinek, T. Lauvaux, B. Lin, M.J. McGill, B. Meadows, N.L. Miles, A.R. Nehrir, J.B. Nowak, M. Obland, C. O'Dell, R.M. P. Fao, S.J. Richardson, D. Richter, A. Roiger, C. Sweeney, J. Walega, P. Weibring, C.A. Williams, M.M. Yang, Y. Zhou, and K.J. Davis. 2021. Atmospheric Carbon and Transport – America (ACT-America) Data Sets: Description, Management, and Delivery. Earth and Space Science 8. https://doi.org/10.1029/2020EA001634